Acta Crystallographica Section F
Structural Biology and Crystallization Communications
ISSN 1744-3091

Nathalie Troffer-Charlier, Vincent Cura, Pierre Hassenboehler, Dino Moras and Jean Cavarelli*

IGBMC (Institut de Génétique et de Biologie Moléculaire et Cellulaire), Département de Biologie et Génomique Structurales, 1 Rue Laurent Fries, Illkirch, F-67404, France; INSERM, U596, Illkirch, F-67400, France; CNRS, UMR7104, Illkirch, F-67400, France; Université Louis Pasteur, Faculté des Sciences de la Vie, Strasbourg, F-67000, France

Correspondence e-mail: cava@igbmc.u-strasbg.fr

Received 26 February 2007
Accepted 13 March 2007

Expression, purification, crystallization and preliminary crystallographic study of isolated modules of the mouse coactivator-associated arginine methyltransferase 1

Coactivator-associated arginine methyltransferase 1 (CARM1) plays a crucial role in gene expression as a coactivator of several nuclear hormone receptors and also of non-nuclear receptor systems. Its recruitment by the transcriptional machinery induces protein methylation, leading to chromatin remodelling and gene activation. $CARM1_{28–507}$ and two structural states of $CARM1_{140–480}$ were expressed, purified and crystallized. Crystals of $CARM1_{28–507}$ belong to space group $P6_222$, with unit-cell parameters $a = b = 136.0$, $c = 125.3$ Å; they diffract to beyond 2.5 Å resolution using synchrotron radiation and contain one monomer in the asymmetric unit. The structure of $CARM1_{28–507}$ was solved by multiple isomorphous replacement and anomalous scattering methods. Crystals of apo $CARM1_{140–480}$ belong to space group $I222$, with unit-cell parameters $a = 74.6$, $b = 99.0$, $c = 207.4$ Å; they diffract to beyond 2.7 Å resolution and contain two monomers in the asymmetric unit. Crystals of $CARM1_{140–480}$ in complex with *S*-adenosyl-L-homocysteine belong to space $P2_12_12$, with unit-cell parameters $a = 74.6$, $b = 98.65$, $c = 206.08$ Å; they diffract to beyond 2.6 Å resolution and contain four monomers in the asymmetric unit. The structures of apo and holo $CARM1_{140–480}$ were solved by molecular-replacement techniques from the structure of $CARM1_{28–507}$.

1. Introduction

Methylation of arginine is a widespread post-translational modification found in eukaryotes and is mediated by the protein arginine methyltransferases (PRMTs). PRMTs are recruited in a variety of biological processes, such as regulation of transcription, translation and DNA repair (for recent reviews, see Bedford & Richard, 2005; Pahlich *et al.*, 2006; Krause *et al.*, 2007). PRMTs transfer the methyl group from *S*-adenosyl-L-methionine (also known as AdoMet or SAM) to the side-chain N atoms of arginine residues to form methylated arginine derivatives and *S*-adenosyl-L-homocysteine (also known as AdoHcy or SAH). To date, at least nine members of the PRMTs (PRMT1–PRMT9) have been found and classified into two major classes (type I and type II PRMTs). Coactivator-associated arginine methyltransferase 1 (CARM1, also known as PRMT4, a type I PRMT) was initially identified as an enhancer of transcriptional activation by nuclear hormone receptors (NRs) by methylation of histone H3 (on Arg3, Arg17 and Arg26) and by protein–protein interactions with the p160 family of coactivators (Chen *et al.*, 1999; for a recent review, see Wysocka *et al.*, 2006). CARM1 is now one of the best characterized secondary coactivators of several NRs such as oestrogen, glucocorticoid, thyroid and androgen receptors. Two essential and synergistic biological functions have been characterized for this protein. CARM1 acts as a methyltransferase on several protein substrates and as a secondary coactivator for several NRs and also non-nuclear receptor systems such as NF-κB (Miao *et al.*, 2006). It has been shown that CARM1 methyltransferase activity is a prerequisite for its coactivator function (Lee *et al.*, 2002). Proteins methylated by CARM1 are vital to gene expression and can be broadly divided into two classes: (i) proteins that are involved in chromatin remodelling [such as histone H3 and the 300 kDa cAMP response element-binding protein (CREB) binding protein (CBP)]

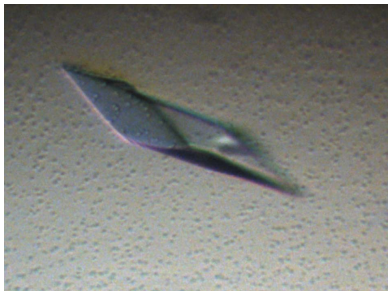

and (ii) proteins which possess RNA-binding properties (such as PABP1, TARPP, HuR and HuD) and splicing factors such as CA510, SAP49, SmB and U1C (Cheng *et al.*, 2007). As a transcriptional coactivator, CARM1 is therefore a key player in the formation of large complexes on gene promoters leading to chromatin remodelling and gene activation.

CARM1 contains 608 amino acids in mouse (and human) and its architecture can be schematically divided into three structural domains. CARM1 is built around a catalytic core domain (residues 150–470 in mouse CARM1; mCARM1) which is very well conserved in sequence (and therefore in structure) among all PRMTs (for recent reviews, see Cheng *et al.*, 2005; Krause *et al.*, 2007). CARM1 possesses two unique additional domains of unknown structure attached at the NH_2-terminal and the COOH-terminal sides of the PRMT active site. Both the NH_2-terminal domain (residues 1–130 in mCARM1) and the COOH-terminal domain (residues 480–608 in mCARM1) have been shown to be required for the coactivator function of human CARM1 (Teyssier *et al.*, 2002). In the first step of a process aimed at understanding on the atomic level the cooperative mechanisms by which CARM1 plays its biological function, two isolated modules of CARM1 ($CARM1_{28–507}$ and $CARM1_{140–480}$) have been expressed using insect cells infected by recombinant baculovirus, purified and crystallized. $CARM1_{28–507}$ (residues 28–507 of mCARM1) contains two structural domains: the NH_2-terminal domain of unknown fold and the PRMT catalytic domain, which is expected to be homologous to other PRMTs. $CARM1_{140–480}$ (residues 140–480 of mCARM1) is slightly larger than the conserved PRMT domain. In the present study, $CARM1_{140–480}$ has been solved in two different biological states: an apo form and a holo form with the *S*-adenosyl-L-homocysteine product bound in the catalytic active site.

2. Methods and results

2.1. Cloning

$CARM1_{28–507}$ was PCR-amplified from the original mouse GST-CARM1 construct (Chen *et al.*, 1999) and cloned in the expression vector pDEST20 (N-terminal GST-tag fusion) using the Gateway system (Invitrogen). The primers used for cloning were 5′-GGG GAC AAG TTT GTA CAA AAA AGC AGG CTT CCT GGT GCC ACG CGG TTC TCA TAT GGC TAC AGT GTC TGT GTT CCC-3′ with an *Nde*I site and a thrombin cleavage site and 5′-GGG GAC CAC TTT GTA CAA GAA AGC TGG GTC AGA TCT TCA GCT GAG ATT ATA GGT GCT TCC-3′ with a *Bgl*II site. The DNA sequence of the amplified module was verified completely by sequencing. Using such a construction, after thrombin cleavage the peptide GSHM will remain at the N-terminal end of the protein, corresponding to a molecular weight of 54 311.8 Da for the isolated module. Recombinant baculovirus was obtained using the Bac-to-Bac Baculovirus Expression System (Invitrogen). DH10Bac competent cells containing the baculovirus genome were transformed with the pDEST20-$CARM1_{28–507}$ plasmid and plated onto LB agar media containing 15 µg ml^{-1} tetracycline, 7 µg ml^{-1} gentamicin, 50 µg ml^{-1} kanamycin, 25 µg ml^{-1} X-Gal and 40 µg ml^{-1} IPTG. Bacmid DNA purified from recombination-positive white colonies was transfected into Sf9 cells using the Lipofectamine reagent (Invitrogen). 10 d after transfection, a small-scale culture was performed to assay for the expression of $CARM1_{28–507}$. The virus was then propagated, titrated and used for large-scale preparations.

$CARM1_{140–480}$ was PCR-amplified from the original mouse GST-CARM1 construct (Chen *et al.*, 1999) and cloned in the expression vector pDEST10 (N-terminal His-tag fusion) using the Gateway system (Invitrogen). The primers used for cloning were 5′-GGG GAC AAG TTT GTA CAA AAA AGC AGG CTT CCT GGT GCC ACG CGG TTC TCA TAT GGA GCG GAC AGA GGA ATC CT-3′ with an *Nde*I site and a thrombin cleavage site and 5′-GGG GAC CAC TTT GTA CAA GAA AGC TGG GTC AGA TCT TCA TGT ACC TGT GTA CCT GAA GAA-3′ with a *Bgl*II site. The DNA sequence of the amplified domain was entirely verified by sequencing. Recombinant baculovirus containing the HisTag-$CARM1_{140–480}$ construct was obtained as described above for GST-$CARM1_{28–507}$.

2.2. Expression and purification

Sf9 cells were grown at 300 K in suspension culture in TNM-FH + 10% foetal calf serum medium (Invitrogen) using spinner flasks (Bellco Biotechnology, USA). 2 l of Sf9 cell culture (at 0.8 × 10^6 cells ml^{-1}) was infected with recombinant GST-$CARM1_{28–507}$ virus with a multiplicity of infection of 1. Cells were harvested 48 h post-infection. Lysis of cells was performed by sonication in 70 ml buffer *A* [50 m*M* Tris–HCl pH 8, 250 m*M* NaCl, 5%(*v*/*v*) glycerol, 5 m*M* β-mercaptoethanol, 0.1%(*w*/*v*) CHAPS] and cellular debris was sedimented by centrifugation of the lysate at 27 000*g* for 30 min. The supernatant was incubated at 277 K for 3 h with 2 ml glutathione Sepharose medium (Amersham Biotech). After a short centrifugation, the supernatant was discarded and the beads were poured into a glass Econo-column (Bio-Rad Laboratories, USA). After two washing steps with 15 ml buffer *A*, 2 ml buffer *A* containing 25 NIH units of thrombin (Sigma) was applied onto the column and digestion was performed overnight at 277 K with gentle shaking. The supernatant containing the CARM1 domain was concentrated with a Centriprep-30 concentrator (Amicon, USA), loaded onto a gel-filtration column (HiLoad 16/60 Superdex S200, Amersham Biotech) and eluted at 1 ml min^{-1} with buffer *B* (20 m*M* Tris–HCl pH 8, 50 m*M* NaCl, 5 m*M* β-mercaptoethanol). The protein eluted as a multimer with an apparent molecular weight of roughly 300 kDa, as estimated after calibration of the gel-filtration column with protein markers (Bio-Rad Laboratories). Fractions containing $CARM1_{28–507}$ were pooled and concentrated to 3.7 mg ml^{-1}. The purity of the protein was verified on a 10% SDS–PAGE gel. 1.5 mg of purified $CARM1_{28–507}$ was typically obtained from 1 l culture.

A similar protocol was used for $CARM1_{140–480}$. Sf9 cells were grown and infected with recombinant HisTag-$CARM1_{140–480}$ as described above for $CARM1_{28–507}$. Lysis of cells was performed in buffer *A* [50 m*M* Tris–HCl pH 7, 250 m*M* NaCl, 5%(*v*/*v*) glycerol, 1 m*M* β-mercaptoethanol, 0.1%(*w*/*v*) CHAPS] and the lysate was clarified by centrifugation (27 000*g* for 30 min) before loading the supernatant onto a Talon metal-affinity column (Clontech). Nonspecifically bound material was removed by washing with buffer *A* supplemented with increasing concentrations of imidazole. $CARM1_{140–480}$ was finally eluted with 150 m*M* imidazole in buffer *A* and dialyzed against buffer *B* (20 m*M* Tris–HCl pH 7, 50 m*M* NaCl, 1 m*M* β-mercaptoethanol). Thrombin cleavage was found to be inefficient and therefore the tobacco etch virus (TEV) cleavage site present in the pDEST10 sequence was used. Therefore, using such a construction, after TEV cleavage an extra peptide GITSLYK-KAGFLVPRGSHM will remain at the N-terminal end of the fusion protein, corresponding to a molecular weight of 40 778.7 Da for $CARM1_{140–480}$. The hexahistidine tag was cleaved by incubation at 303 K for 3 h with 25 µg TEV protease per milligram of protein. The protein solution was concentrated with a Centriprep YM-30 concentrator (Millipore) and applied onto a gel-filtration column (HiLoad 16/60 Superdex S200, Amersham Biotech) equilibrated in buffer *B*. Elution fractions were combined, concentrated to

2 mg ml^{-1} and used for crystallization trials. The purity of the protein was followed at each step by SDS–PAGE. 1 mg of purified CARM1$_{140–480}$ was typically obtained from 1 l culture.

2.3. Buffer optimization prior to crystallization

In order to determine an optimal buffer that gives the most homogenous and monodisperse protein, the screening-solubility method described by Jancarik *et al.* (2004) was implemented and used. CARM1$_{28–507}$ was concentrated (to 2 mg ml^{-1}) in 20 m*M* Tris–HCl pH 8, 50 m*M* NaCl, 5 m*M* β-mercaptoethanol. 24 different buffers, ranging from pH 3 to pH 9.5, were used to set up vapour-diffusion experiments. After one night at 295 K, clear drops (6 µl) were diluted with 8 µl reservoir solution and dynamic light-scattering analysis was performed using a DynaPro-MS (Protein Solutions, USA). The polydispersity of the protein was minimal in sodium acetate pH 4.5 buffer (C_p/R_h = 15%). Therefore, prior to crystallization trials the protein was dialyzed against 25 m*M* sodium acetate pH 4.5, 1 m*M* tris(2-carboxyethyl)phosphine (TCEP).

Optimal buffers for CARM1$_{140–480}$ were found using a similar protocol as described above for CARM1$_{28–507}$. The polydispersity of CARM1$_{140–480}$ was minimal at pH 7 in four different buffers (C_p/R_h = 15%; imidazole, sodium/potassium phosphate, ammonium acetate, Tris–HCl). For crystallization trials, the protein was concentrated (to 2 mg ml^{-1}) in 20 m*M* Tris–HCl pH 7, 50 m*M* NaCl, 1 m*M* β-mercaptoethanol.

2.4. Crystallization and data collection

2.4.1. CARM1$_{28–507}$. Crystallization conditions were screened using commercially available kits by the sitting-drop vapour-diffusion method in 96-well CrystalQuick plates (Greiner Bio-One), employing a Tecan robot. Initial hits were obtained in the MembFac screen (Hampton Research, USA). After optimization, hexagonal shaped crystals (200 × 60 × 50 µm; Fig. 1) grew in a few days in hanging drops made by mixing 1 µl protein solution (3.7 mg ml^{-1}) and 1 µl reservoir solution consisting of 5–9%(*v*/*v*) MPD, 100 m*M* sodium citrate pH 5.6, 100 m*M* NaCl or LiCl, 0–200 m*M* Li_2SO_4 and 100 m*M* benzamidine chloride. Drops were equilibrated against 0.5 ml reservoir solution at 277 K. Crystals were flash-frozen in liquid nitrogen after a brief transfer to 5 µl reservoir solution containing 20%(*v*/*v*) MPD as a cryoprotectant and were stored in liquid nitrogen. X-ray diffraction data were collected using a single cryocooled (100 K) crystal on beamline ID29 at the European Synchrotron Radiation Facility (ESRF). The best crystals diffracted to beyond 2.5 Å and a complete data set was obtained between 50 and 2.55 Å resolution from 240 frames of 0.5° oscillation (exposure time of 1 s per oscillation with an attenuated beam, a crystal-to-detector distance of 418 mm and a Q315 CCD detector from ADSC). The data were indexed, processed and scaled with *HKL*-2000 (Otwinowski & Minor, 1997). The crystals belong to the hexagonal space group $P6_222$, with unit-cell parameters $a = b = 136.0$, $c = 125.3$ Å (Table 1). The asymmetric unit contains one molecule, with a corresponding crystal volume per protein weight of 3.08 Å^3 Da^{-1} and a solvent content of 60% (assuming a partial specific volume of 0.74 cm^3 g^{-1}). Data-collection statistics are summarized in Table 1.

Table 1
Data-collection statistics for CARM1$_{28–507}$ and apo and holo CARM1$_{140–480}$.

Values in parentheses are for the highest resolution shell.

	CARM1$_{28–507}$	CARM1$_{140–480}$	CARM1$_{140–480}$ + AdoHcy
Beamline station (ESRF)	ID29	ID14-4	ID29
Wavelength (Å)	0.9199	0.9794	0.9537
Resolution range (Å)	50–2.55 (2.63–2.55)	50–2.8 (2.9–2.8)	50–2.65 (2.74–2.65)
Space group	$P6_222$	$I222$	$P2_12_12$
Unit-cell parameters			
a (Å)	136.0	74.6	74.6
b (Å)	136.0	99.0	98.65
c (Å)	125.3	207.4	206.08
Measured reflections	263616	120102	293441
Unique reflections	22679	19042	45632
Completeness (%)	99.1 (99.4)	99.1 (96.5)	97.0 (94.6)
$I/\sigma(I)$	38.3 (6.1)	27.3 (4.0)	22.8 (3.9)
Redundancy	11.6 (11.5)	6.3 (4.9)	6.4 (5.8)
R_{merge}† (%)	6.4 (25.8)	6.1 (25.7)	8.6 (29.7)

† R_{merge} indicates the agreement of individual reflections over the set of unique averaged reflections: $R_{merge} = \sum_h \sum_i |\langle I_h\rangle - I_{h,i}| / \sum_h \sum_i I_{h,i}$, where $I_{h,i}$ is the ith observed intensity of a measured reflection of Miller index h and $\langle I_h\rangle$ is the average intensity for this unique reflection.

The structure of CARM1$_{28–507}$ was solved by the multiple isomorphous replacement and anomalous scattering methods from two heavy-atom derivatives (trimethyllead acetate and xenon). Because of the presence of sodium citrate in the mother liquor, crystals were not soaked with heavy atoms directly in the crystallization drops. For the lead derivative, native crystals were first transferred into pre-equilibrated drops containing 1 µl reservoir solution [20%(*v*/*v*) MPD, 100 m*M* HEPES pH 7.5, 100 m*M* LiCl, 100 m*M* Li_2SO_4] and 1 µl protein solution (3.4 mg ml^{-1} in 25 m*M* sodium acetate pH 4.5). 1 µl of a solution of 10 m*M* trimethyllead acetate was then added to the drops and crystals were allowed to incubate for 30 min. Soaked crystals were flash-cooled in liquid nitrogen. X-ray diffraction data were collected using a single cryocooled (100 K) crystal on beamline ID14-4 at the ESRF. A complete anomalous data set was obtained between 50 and 3.2 Å resolution from 180 frames of 1° oscillation (exposure time of 2 s per oscillation

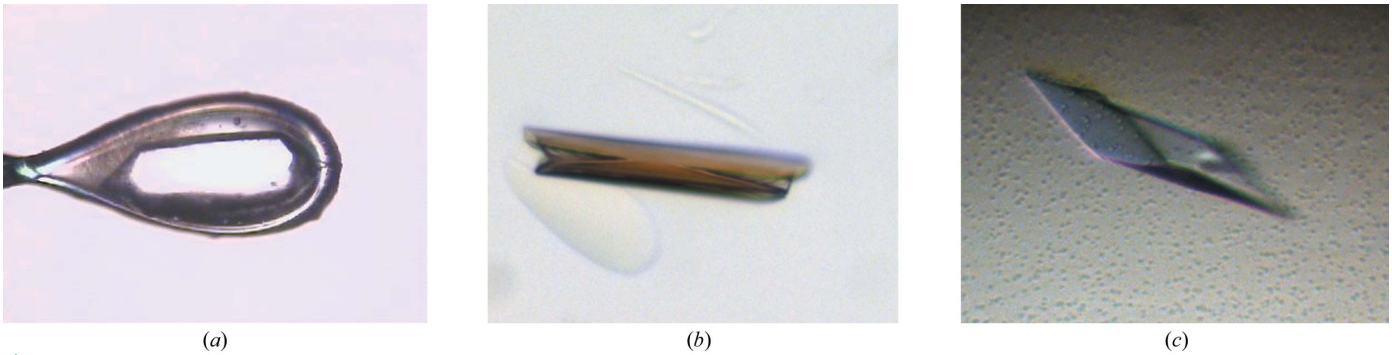

(*a*) (*b*) (*c*)

Figure 1
Crystals of isolated modules of mouse CARM1. (*a*) CARM1$_{28–507}$ (200 × 60 × 50 µm), (*b*) apo CARM1$_{140–480}$ (250 × 40 × 40 µm), (*c*) CARM1$_{140–480}$–AdoHcy (200 × 120 × 40 µm).

with an attenuated beam, a crystal-to-detector distance of 474 mm, a wavelength of 0.9395 Å and a Q315 CCD detector). For the xenon derivative, after a brief transfer in the cryobuffer, crystals were exposed to 8×10^5 Pa xenon for 5 min using the Oxford Cryosystems Xcell available at beamline ID23 of the ESRF. After decompression, crystals were flash-cooled in liquid nitrogen. X-ray diffraction data were collected using a single cryocooled (100 K) crystal on beamline ID23 at the ESRF. A complete data set was obtained between 50 and 3.1 Å resolution from 180 frames of 1° oscillation (exposure time of 1 s per oscillation with an attenuated beam, a wavelength of 1.009 Å, a crystal-to-detector distance of 444 mm and a Q315 CCD detector).

2.4.2. Apo CARM1$_{140–480}$. Crystallization conditions were screened using commercially available kits by the sitting-drop vapour-diffusion method in 96-well CrystalQuick plates (Greiner Bio-One). Initial hits were obtained with the JCSG+ screen from Qiagen. After optimization, rod-shaped crystals (250 × 40 × 40 µm) suitable for X-ray diffraction grew in two weeks in hanging drops made by mixing 1 µl protein solution at 2 mg ml^{-1} and 1 µl reservoir solution consisting of 19%(*v*/*v*) PEG 3350, 0.15 *M* sodium malate pH 7. Drops were equilibrated against 0.5 ml reservoir solution at 297 K. Fully grown crystals were stabilized by the addition of 0.1 *M* arginine to the drop. Prior to X-ray exposure, crystals were flash-cooled in liquid nitrogen after a short transfer into 5 µl reservoir solution supplemented with 20%(*v*/*v*) PEG 400 as a cryoprotectant. X-ray diffraction data were collected using a single cryocooled (100 K) crystal on beamline ID14-4 at the ESRF. The best crystals diffracted to beyond 2.7 Å and a complete data set was obtained between 50 and 2.8 Å resolution from 360 frames of 0.5° oscillation (exposure time of 1 s per oscillation with an attenuated beam, a crystal-to-detector distance of 421 mm and a Q315 CCD detector). The data were indexed, processed and scaled with *HKL*-2000 (Otwinowski & Minor, 1997). The crystals belong to the orthorhombic space group *I*222, with unit-cell parameters $a = 74.6$, $b = 99.0$, $c = 207.4$ Å (Table 1). The asymmetric unit contains two molecules, with a corresponding crystal volume per protein weight of 2.35 Å^3 Da^{-1} and a solvent content of 47.6% (assuming a partial specific volume of 0.74 cm^3 g^{-1}). Data-collection statistics are summarized in Table 1.

2.4.3. CARM1$_{140–480}$ in complex with the cofactor product AdoHcy. Prior to crystallization trials, protein was incubated with 0.4 m*M* *S*-adenosyl-L-homocysteine (AdoHcy), the cofactor product of the protein arginine *N*-methyltransferase reaction. Crystallization hanging drops were set up by mixing 1 µl protein solution at 1.5 mg ml^{-1} and 1 µl reservoir solution consisting of 14%(*w*/*v*) PEG 3350, 50 m*M* arginine, 0.15 *M* sodium malate pH 7 and were equilibrated against 0.5 ml reservoir solution. Crystals (200 × 120 × 40 µm) grew in a few days at 290 K. Prior to X-ray exposure, crystals were flash-cooled in liquid nitrogen after a short transfer into 5 µl reservoir solution supplemented with 20%(*v*/*v*) PEG 400 as a cryoprotectant. X-ray diffraction data were collected using a single cryocooled (100 K) crystal on beamline ID29 at the ESRF. The best crystals diffracted to beyond 2.6 Å and a complete data set was obtained between 50 and 2.65 Å resolution from 360 frames of 0.5° oscillation (exposure time of 1 s per oscillation with an attenuated beam, a crystal-to-detector distance of 412 mm and a Q315 CCD detector). The data were indexed, processed and scaled with *HKL*-2000 (Otwinowski & Minor, 1997). The crystals belong to the orthorhombic space group $P2_12_12$, with unit-cell parameters $a = 74.6$, $b = 98.65$, $c = 206.08$ Å (Table 1). The asymmetric unit contains four molecules, with a corresponding crystal volume per protein weight of 2.33 Å^3 Da^{-1} and a solvent content of 47.3% (assuming a partial specific volume of 0.74 cm^3 g^{-1}). Data-collection statistics are summarized in Table 1.

3. Structure determination

The structure of CARM1$_{28–507}$ has been solved by multiple isomorphous replacement and anomalous scattering methods from two heavy-atom derivatives (lead and xenon) using *SOLVE* (Terwilliger & Berendzen, 1999; details to be published elsewhere). The phasing process allowed the determination of the correct space group ($P6_222$ *versus* $P6_422$).

The structures of CARM1$_{140–480}$ alone and in complex with the cofactor product AdoHcy were solved by molecular-replacement methods using the corresponding isolated domain extracted from the previously solved CARM1$_{28–507}$ structure as a probe with *MOLREP* (Collaborative Computational Project, Number 4, 1994). Despite the fact that the crystals of the apo and holo (in the presence of AdoHcy) forms of CARM1$_{140–480}$ were obtained from very similar mother-liquor conditions, they correspond to two different space groups ($P2_12_12$ for the holo form and *I*222 for the apo form), but nevertheless with very similar unit-cell parameters (see Table 1 for details). The structure determinations of the two crystal forms reveal that the apo crystal form contains one dimer of CARM1$_{140–480}$ in the asymmetric unit, while the holo crystal form contains two dimers in the asymmetric unit. In the $P2_12_12$ holo form, the two dimers are related by a noncrystallographic fractional translation of (∼0.47, 0.50, 0.50), resulting in a pseudo-*I*222 packing. The molecular switch responsible for the crystal transition will be described elsewhere.

We thank members of the ESRF–EMBL Joint Structural Biology Group for use of the ESRF beamline facilities and help during data collection. We are indebted to the baculovirus common resources of the IGBMC for recombinant virus productions. We thank the members of the structural biology platform of our department for technical assistance. The work described here was supported by funds from Association pour la Recherche sur le Cancer (contracts Nos. 3230 and 3910) and the European Commission as SPINE2 complexes contract No. LSHG-CT-2006-031220.

References

Bedford, M. T. & Richard, S. (2005). *Mol. Cell*, **18**, 263–272.
Chen, D., Ma, H., Hong, H., Koh, S. S., Huang, S. M., Schurter, B. T., Aswad, D. W. & Stallcup, M. R. (1999). *Science*, **284**, 2174–2177.
Cheng, D., Cote, J., Shaaban, S. & Bedford, M. T. (2007). *Mol. Cell*, **25**, 71–83.
Cheng, X., Collins, R. E. & Zhang, X. (2005). *Annu. Rev. Biophys. Biomol. Struct.* **34**, 267–294.
Collaborative Computational Project, Number 4 (1994). *Acta Cryst.* D**50**, 760–763.
Jancarik, J., Pufan, R., Hong, C., Kim, S.-H. & Kim, R. (2004). *Acta Cryst.* D**60**, 1670–1673.
Krause, C. D., Yang, Z. H., Kim, Y. S., Lee, J. H., Cook, J. R. & Pestka, S. (2007). *Pharmacol. Ther.* **113**, 50–87.
Lee, Y. H., Koh, S. S., Zhang, X., Cheng, X. & Stallcup, M. R. (2002). *Mol. Cell. Biol.* **22**, 3621–3632.
Miao, F., Li, S., Chavez, V., Lanting, L. & Natarajan, R. (2006). *Mol. Endocrinol.* **20**, 1562–1573.
Otwinowski, Z. & Minor, W. (1997). *Methods Enzymol.* **276**, 307–326.
Pahlich, S., Zakaryan, R. P. & Gehring, H. (2006). *Biochim. Biophys. Acta*, **1764**, 1890–1903.
Terwilliger, T. C. & Berendzen, J. (1999). *Acta Cryst.* D**55**, 849–861.
Teyssier, C., Chen, D. & Stallcup, M. R. (2002). *J. Biol. Chem.* **277**, 46066–46072.
Wysocka, J., Allis, C. D. & Coonrod, S. (2006). *Front. Biosci.* **11**, 344–355.